# On the Effect of the Boundary Conditions and the Collision Model on Rarefied Gas Flows

M. Vargas[a], S. Stefanov[a] and D. Valougeorgis[b]

[a]*Institute of Mechanics, Bulgarian Academy of Sciences, Acad. G. Bonchev Str., Block 4, Sofia 1113, Bulgaria*
[b]*Department of Mechanical Engineering, University of Thessaly, Pedion Areos, 38334, Volos, Greece*

**Abstract.** In this work, the effect of the gas-surface interaction law and of the intermolecular collision model is examined by solving, using the DSMC method, the heat transfer problem between parallel plates and the non-isothermal Poiseuille flow problem. In the former one the Cercignani-Lampis model is applied to analyze the influence of the gas-surface interaction parameters, while in the latter one a comparison between the results obtained by implementing the Hard Sphere, Variable Hard Sphere, Variable Soft Sphere and Maxwellian models is performed. Calculations have been carried out for several values of the Knudsen number, temperature ratio and Froude number. A comparison between the DSMC and the corresponding discrete velocity results yields very good agreement between the two approaches. Finally, the convergence behavior of a Bernoulli trials based scheme, which allows the use of a smaller number of particles per cell, and the No Time Counter are compared for different sampling sequences.

**Keywords:** boundary conditions, interaction models, heat transfer, DSMC, Bernoulli trials.
**PACS:** 05.10.Ln

## INTRODUCTION

The DSMC method proposed by Bird [1] is used to study i) the one-dimensional heat transfer (Fourier flow) problem and ii) adding a force parallel to the walls, the Poiseuille flow with non-isothermal walls. The influence of the boundary conditions on the heat flux is analyzed for the Fourier flow problem by using the Cercignani-Lampis (CLL) model [2]. This model, compared to the well-known specular-diffuse reflection model, provides an improved physical meaning [3]. The implementation of the CLL model in the DSMC has been described by Lord [4]. A comparison between the DSMC and the corresponding discrete velocity results [5] in the whole range of Knudsen number is included.

The influence of different intermolecular potentials (Hard Sphere, Variable Hard Sphere, Variable Soft Sphere and Maxwellian) on the calculation of the heat flux is analyzed for the acceleration driven flow between plates with non-isothermal walls. In addition, the effect of all the parameters involved in this problem (Knudsen number, temperature ratio and Froude number) is investigated.

Finally, the convergence behavior of a Bernoulli trials based scheme, which has been previously used [6] for 3D calculations, is implemented. The behavior of this more advanced scheme is compared with the typical No Time Counter scheme and several sampling performances are included in a similar way as presented in [7].

## PROBLEM FORMULATION

### Plane Fourier Flow

The one-dimensional plane Fourier flow problem deals with the heat transfer through a gas confined between two infinite stationary parallel plates maintained at different temperatures. The plates are at $y = 0$ and $y = L$ with temperatures $T_C = T_0 (1 - \Delta T)$ and $T_H = T_0 (1 + \Delta T)$ respectively as shown in Figure 1 (left). The initial state of the gas is in equilibrium at reference pressure and temperature $P_0$ and $T_0$, with a reference number density $n_0 = P_0/(RT_0)$

and a reference Knudsen number $Kn_0 = \lambda_0/L$, where $\lambda_0$ is the mean free path, which is defined for hard sphere particles as $(\sqrt{2}\pi d^2 n_0)^{-1}$, with $d$ being the diameter of the particles and $R$ the gas constant.

To render the problem dimensionless, we normalize the position by $L$, the temperatures by $T_0$, the velocities by the most probable molecular speed $v_0 = \sqrt{2R_m T_0}$, the number density by $n_0$ and the heat flux $q_y$ by $(n_0 m v_0^3)$. Here $R_m$ is the specific gas constant and $m$ is the molecular mass.

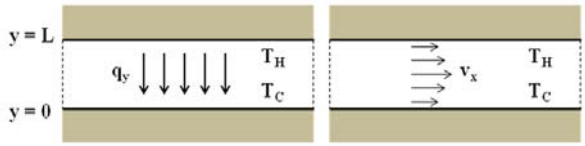


**FIGURE 1.** Schematic diagram of the plane Fourier flow (left) and non-isothermal Poiseuille flow (right)

## Plane Acceleration-Driven Flow with Temperature Difference

The one-dimensional plane non-isothermal Poiseuille flow consists of the movement of a gas between two parallel plates maintained at different temperatures $T_H$ and $T_C$ due to the effect of a pressure difference along the channel. It can be described schematically also by Figure 1 (right), but adding a pressure difference parallel to the plates. The implementation of this flow was done considering a very short region of the parallel plates, so that we could assume that the pressure gradient in this region is constant, and with periodic conditions at the boundaries perpendicular to the walls in order to simulate a fully developed flow. The implementation consisted of an acceleration-driven flow, where a constant body force parallel to the plates ($F = mg$) acts on every particle of the domain. This acceleration can easily be related to the pressure gradient $dP/dx$ by using the expression:

$$g = \frac{1}{\rho}\frac{dP}{dx} \tag{1}$$

For this case we can obtain an additional non-dimensional parameter, the Froude number $Fr = \dfrac{v_0^2}{g\,L}$.

## Cercignani – Lampis Boundary Conditions

The Cercignani-Lampis model (CLL) is used in this work to compute the gas-surface interactions. The CLL model contains two adjustable parameters, namely the normal energy accommodation coefficient, $\alpha_n$, and the tangential momentum accommodation coefficient, $\sigma_t$. The first one, $\alpha_n$, can range from 0 to 1 and is related to the part of kinetic energy corresponding to the normal velocity, while the latter, $\sigma_t$, can range from 0 to 2 and is related to the tangential momentum. Besides, the tangential energy accommodation coefficient can be defined as $\alpha_t = \sigma_t (2-\sigma_t)$. The scattering kernel consists of three parts, one for each of the velocity components, and represents the probability of a particle with incident velocity $\xi'$ to be reflected with $\xi$.

The implementation of the model in DSMC simulations is well described by Lord [4]. First, the components of the pre-collision velocity $(\xi'_x, \xi'_y, \xi'_z)$ are expressed in a local coordinate system parallel to the incident velocity vector of the molecule obtaining $(u', v', 0)$, where $u' = \sqrt{\xi_x'^2 + \xi_z'^2}$ and $v' = \xi'_y$. The value in the local coordinate system of the tangential post-collision velocity components $u$ and $w$ can be sampled as follows:

$$\theta = 2\pi R_{f1}; \qquad r = \left[-\sigma_t\left(2-\sigma_t\right)\ln\left(R_{f2}\right)\right]^{1/2}; \qquad u = \left(1-\sigma_t\right)u' + r\cos\theta; \qquad w = r\sin\theta \tag{2}$$

The value of the normal velocity component $v$ can be sampled:

$$\theta = 2\pi R_{f3}; \qquad r = \left[-\alpha_n \ln\left(R_{f4}\right)\right]^{1/2}; \qquad v = \left(r^2 + \left(1-\alpha_n\right)\left|v'\right|^2 + 2r\sqrt{\left(1-\alpha_n\right)\left|v'\right|}\cos\theta\right)^{1/2} \tag{3}$$

It is important to mention that all velocities are referred to the most probable velocity at the wall temperature $\sqrt{2kT_w}$. Finally, the velocity vector is transformed into the global coordinate system.

## Molecular Interaction Models

There are several collision models which describe different kinds of interactions between the particles. The inverse power law model is based on the assumption that the repulsive force between the particles is inversely proportional to $1/r^{\eta}$. The dependence of the viscosity and thermal conductivity with temperature is proportional to $T^{\omega}$, where

$$\omega = \frac{1}{2} + \nu = \frac{1}{2}\frac{\eta+3}{\eta-1} \tag{4}$$

According to this, the dependence is proportional to $T^{1/2}$ and to $T$ for hard sphere ($\eta \to \infty$) and Maxwellian interaction ($\eta = 5$) respectively. One of the drawbacks of the HS model is that the cross-section is independent of the relative translational energy ($E_t$) in the collision, which is not realistic. Therefore, a variable cross-section is required to match the powers of the order of 0.75 which are characteristic of real gases.

This led to the definition of the Variable Hard Sphere (VHS) model which represents a hard sphere molecule whose diameter $d$ is function of the relative molecular velocity $c_r$.

$$\frac{\sigma_T}{\sigma_{T,ref}} = \left(\frac{d}{d_{ref}}\right)^2 = \left(\frac{c_r}{c_{r,ref}}\right)^{-2\nu} \tag{5}$$

where $\sigma_{T,ref}$, $d_{ref}$ and $c_{r,ref}$ are reference values. In the VHS model, the ratio of the momentum to the viscosity cross-section follows the HS value. However, this is a deficiency because the ratio varies with the power law in the case of the inverse power law model, and the real gas values are different from HS values.

This led to the definition [8] of the VSS model, where the deflection angle $\chi$ is given by:

$$\chi = 2\cos^{-1}\left[\left(b/d\right)^{1/\alpha}\right] \tag{6}$$

The VSS model matches the HS model when $\alpha$ is equal to 1 and $\nu$ is equal to 0 ($\omega = ½$). The reference molecular diameter is related by equation (7) to the reference viscosity for all the cases and it is defined by:

$$d_{ref}^{\,2} = \frac{5(\alpha+1)(\alpha+2)\left(\frac{mkT_{ref}}{\pi}\right)^{1/2}}{4\alpha(5-2\omega)(7-2\omega)\mu_{ref}} \tag{7}$$

Here, the following expressions for the components of the postcollision relative velocity have been used:

$$u_r^{\,*} = \cos\chi\, u_r + \sin\chi \sin\varepsilon \left(v_r^{\,2} + w_r^{\,2}\right)^{1/2} \tag{8}$$

$$v_r^{\,*} = \cos\chi\, v_r - \sin\chi\left(c_r\, w_r \cos\varepsilon + u_r\, v_r \sin\varepsilon\right)\Big/\left(v_r^{\,2} + w_r^{\,2}\right)^{1/2} \tag{9}$$

$$w_r^{\,*} = \cos\chi\, w_r + \sin\chi\left(c_r\, v_r \cos\varepsilon - u_r\, w_r \sin\varepsilon\right)\Big/\left(v_r^{\,2} + w_r^{\,2}\right)^{1/2} \tag{10}$$

## RESULTS AND DISCUSSIONS

### Gas-Surface Interaction in the Fourier Flow

The influence of the gas-surface interaction parameters involved in the CLL model on the heat transfer for pure planar Fourier flow is shown in Figure 2 for $\Delta T = 0.1$ and the HS model. In particular, the heat flux is plotted versus each accommodation coefficient, keeping the other constant and equal to unity. It can be seen that the influence of the accommodation coefficients is high for large Knudsen numbers, but lower when the Knudsen number decreases. This can be explained taking into account that as Knudsen is increased the collisions with the walls are dominant as the whole domain is contained within the Knudsen layers. The opposite happens when the Knudsen number is decreased and the collision between the molecules becomes more important than the collision with the boundaries.

Besides, a symmetric dependence of the heat flux on $\sigma_t$ around $\sigma_t = 1$ can be observed. This symmetry is understandable since in pure Fourier flow there is no macroscopic movement of the gas, where specular reflection has the same global effect as backscattering. On the contrary, the heat flux increases monotonically with $\alpha_n$.

In addition, calculations of the heat flux for the plane Fourier flow for diffuse boundary conditions were carried out in order to compare the DSMC results with those obtained using the discrete velocity method [5]. The simulations were done for different rarefaction conditions, from the free molecular regime until the continuum flow

regime, and for the case of $\Delta T = 2$ ($T_H/T_C = 3$). The results are shown in Table 1 for different Knudsen numbers. The results between both approaches are in very good agreement.

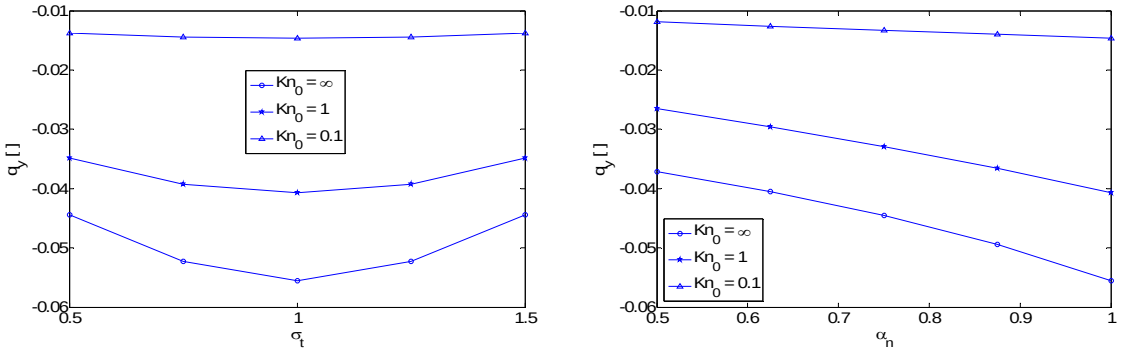


**FIGURE 2.** Heat flux dependence on the tangential momentum accommodation coefficient $\sigma_t$ keeping $\alpha_n = 1$ (left) and on the normal energy accommodation coefficient $\alpha_n$ keeping $\sigma_t = 1$ (right).

**TABLE 1.** Heat flux in the whole range of rarefaction and $\Delta T = 2$ ($T_H/T_C = 3$) obtained by DSMC and DVM.

| $\frac{\sqrt{\pi}}{2}\frac{1}{Kn}$ | **0.0** | **0.15** | **1.5** | **15** | **150** |
|---|---|---|---|---|---|
| **DSMC** | $2.534\cdot10^{-1}$ | $2.373\cdot10^{-1}$ | $1.674\cdot10^{-1}$ | $4.891\cdot10^{-2}$ | $6.214\cdot10^{-3}$ |
| **DVM** | $2.534\cdot10^{-1}$ | $2.371\cdot10^{-1}$ | $1.662\cdot10^{-1}$ | $4.837\cdot10^{-2}$ | $6.015\cdot10^{-3}$ |

## Molecular Interaction Models in the Poiseuille Flow with Heat Transfer

In Figure 3 temperature distributions between the plates are shown for various flow parameters. In each case results for all four implemented potentials are provided. It is seen that in each of Figures 3a, 3c and 3d, with $Kn$ = 0.1, the corresponding temperature distributions are very close. Significant differences appear only for $Kn$ = 0.01 (Figure 3b), as the intermolecular collisions become predominant over the collisions with the walls and the flow velocity increases when the $Kn$ is decreased and the $Fr$ remains constant.

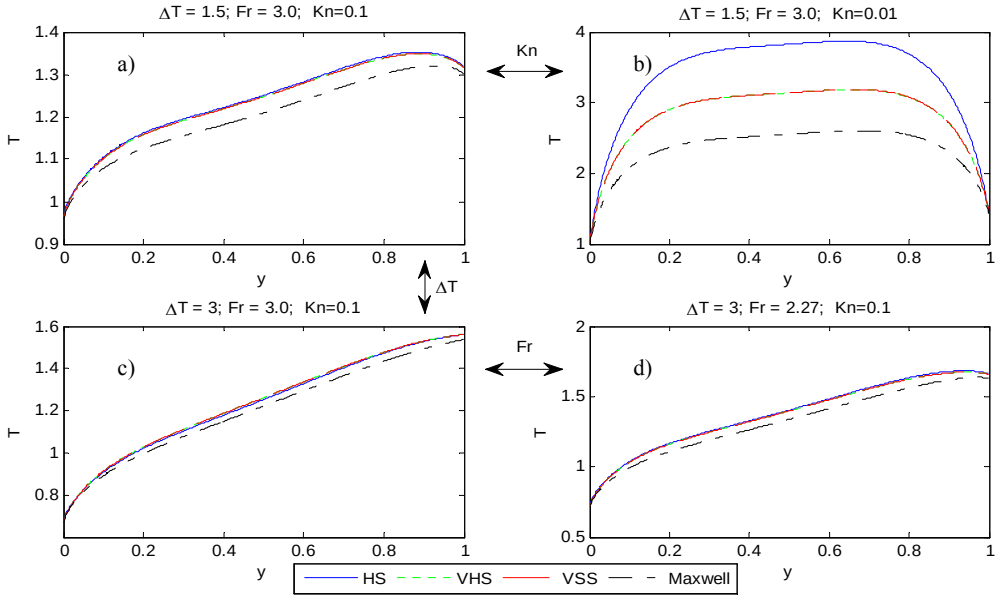


**FIGURE 3.** Temperature dependence on the chosen molecular interaction model for the shown values of $Kn$, $Fr$ and $T_H/T_C$.

Also by observing Figures 3a, 3c and 3d, where the Knudsen number is the same, the effect of changing the temperature ratio and the Froude number can be examined. More specifically, at higher temperature ratio and Froude number (Figure 3d), the temperature distribution is monotonic while, as the temperature ratio and the Froude number are reduced, it becomes non-monotonic with a peak close to the hot wall (Figures 3a and 3d).

The corresponding results for the heat flux are shown in Figure 4. As expected, the heat transfer increases when the temperature ratio increases. It can be seen that in Figure 4c the heat flux is always negative, while in Figure 4a is positive in part of the domain. This is explained by monitoring the corresponding temperature profiles. The influence of the Froude number can be analyzed by comparing Figure 4c and 4d. When the *Fr* is decreased, the heat flux in the central region of the domain is slightly increased as well as the difference between the heat flux in the hot and in the cold wall. Regarding the role of the applied intermolecular model, its influence is negligible at high Knudsen. In general, the differences in the results for the various models increase as the Knudsen number decreases and the temperature ratio increases. The differences between the models appear to be larger in the central region of the channel in the temperature profiles, while for the heat transfer a bigger difference is seen near the walls. The largest discrepancies appear between the HS and Maxwellian models, with the Maxwellian model being the one which produces the highest value for the heat flux. The differences between the VHS and VSS models are quite small for the cases analyzed in this work.

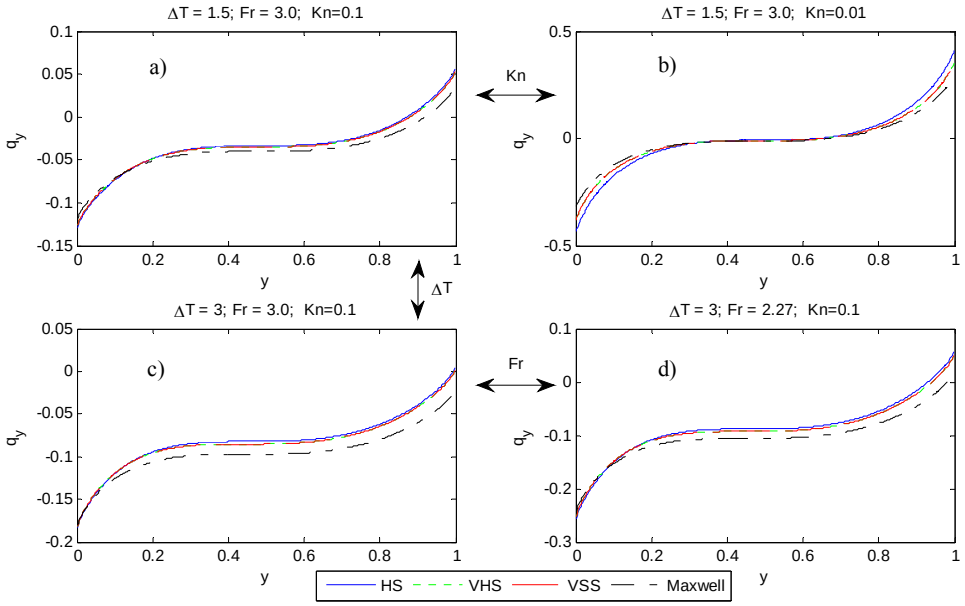


**FIGURE 4.** Heat flux dependence on the chosen molecular interaction model for the shown values of *Kn*, *Fr* and $T_H/T_C$.

## No Time Counter and Bernoulli Trial Schemes

The convergence behavior of a Bernoulli trials based scheme [6] is investigated for different sampling performances and compared with the widely used No Time Counter scheme (NTC) proposed by Bird [1].

In the NTC scheme the maximum number of collision pairs is calculated at the beginning and then pairs are selected randomly and the collisions are computed with a certain probability. Instead, in the Bernoulli Trials based scheme (BT) all possible collision pairs within the cell are chosen to be collided with a certain probability which is proportional, as in the case of NTC, to the total cross section and the relative velocity. By computing all possible pairs, the repeated collisions, which can lead in certain conditions to wrong results, are avoided. The computational cost of the BT scheme is proportional to $N^2$, being $N$ is the average number of particles per cell, in contrast to the NTC scheme with proportionality to $N$. However, the BT scheme allows the use of a small number of particles per cell, keeping the same accuracy as the NTC scheme. Furthermore, in order to allow collisions between particles of neighboring cells, a dual grid was introduced. The binary collisions in each cell are calculated in the original grid for a time interval $\Delta t/2$ and then in the shifted grid – shifted $\Delta x/2$ in x- and y-direction – for the other $\Delta t/2$ without moving the particles. Then all the particles in the domain are moved at a distance proportional to their new velocities without colliding during $\Delta t$.

In this section, three different sampling performances were analyzed for each scheme:

- For the NTC scheme collision-sample-move (CSM), collision-move-sample (CMS) and collision-sample-move-sample (CSMS).
- For the BT scheme collision1-collision2-move-sample (C1C2MS), collision1-collision2-sample-move (C1C2SM) and the symmetric collision1-sample-collision2-move (C1SC2M).

The study case chosen for this aim was the Fourier flow defined above with purely diffuse walls and with reference pressure and temperature of the hard-sphere-like gas $P_0$ and $T_C$ and with $\Delta T = 0.1T_0$. The reference Knudsen is $Kn_0 = 0.09$ and the reference heat flux for these cases is $q_{ref} = n_0 m v_{0C}$, where $v_{0C} = \sqrt{2R_m T_C}$ .

The results presented here represent the time discretization errors of the different schemes for two different values of the mean number of particles per cell.

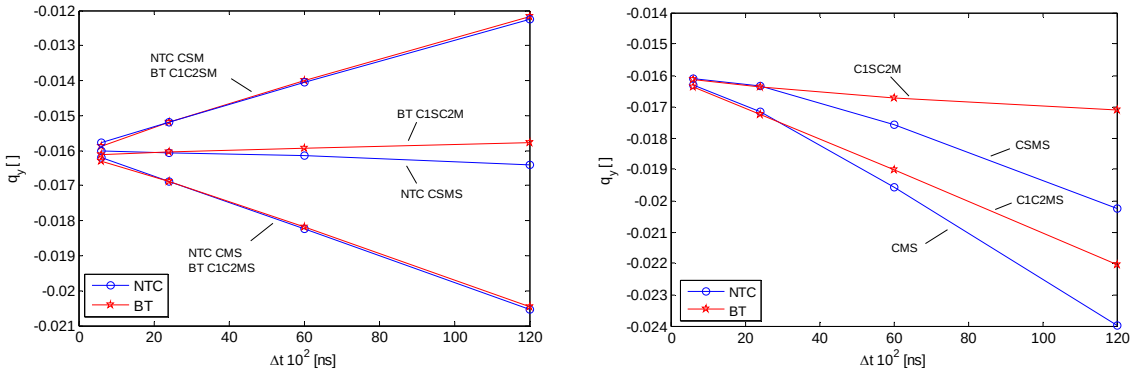


**FIGURE 5.** Heat flux versus time step for the different schemes (NTC and BT) and sampling procedures. The simulations were performed dividing the domain in 200 cells and using (left) 50 and (right) 2 particles per cell as average.

The results presented show the dependence of the heat flux on the selected scheme. When the average number of particles per cell is big enough (Figure 5 left), the behavior of both schemes (NTC and BT) are very similar. With two of the methods, NTC with double sampling (CSMS) and BT with symmetric sampling (C1SC2M), the heat flux deviates slightly from the converging value when the time step is increased. The value of the heat flux is overpredicted for the BT with symmetric sampling, while for NTC with double sampling is underpredicted. For the other four DSMC models the heat flux converge to the same value as the previous methods for small time steps, but it deviates significantly when the time step increases.

However, if the average number of particles per cell is drastically reduced (Figure 5 right), it turns out that only the BT scheme with symmetric sampling can cope with a very low number of particles per cell and the increase of the time step. The NTC with double sampling gives the same value of the heat flux for small time steps, but they deviate when this time step starts increasing. The other single-sampling methods describe a similar but more pronounced tendency as with using a large number of particles per cell.

## ACKNOWLEDGMENTS

The research leading to these results has received funding from the European Community's Seventh Framework Programme (ITN - FP7/2007-2013) under grant agreement n° 215504.

## REFERENCES

1. G. A. Bird, *Molecular Gas Dynamics and the Direct Simulation of Gas Flows*, Oxford, Clarendon, 1994.
2. C. Cercignani, M. Lampis. *Transp. Theory and Stat. Physics*, **1**, 101-114 (1971).
3. F. Sharipov. *European Journal of Mechanics B/Fluids* **21**, 113-123 (2002).
4. R. G. Lord. *Phys. Fluids A*, **3**, 706-710 (1991).
5. S. Pantazis, D. Valougeorgis. *Heat transfer between parallel plates via kinetic theory in the whole range of the Knudsen number*. 5th European Thermal-Sciences Conference, Eindhoven, 2008.
6. S. Stefanov, V. Roussinov, C. Cercignani. *Phys. Fluids* **19**, 124101 (2007).
7. M. A. Gallis, J. R. Torczynski, D. J. Rader, M. Tij, A. Santos. *Phys. Fluids* **18**, 017104 (2006).
8. K. Koura, H. Matsumoto. *Phys. Fluids A*, **3**, 2459-2465 (1991).